



---

## A Computational Evaluation for Hazardous Emissions of Non-premixed Shale Gas Combustion

Suat OZTURK

DERAC, ZonguldakBülent Ecevit University, 67100, Zonguldak, Turkey

---

**Abstract** Two dimension numerical investigation of the non-premixed combustion of shale gas and air in the cylindrical combustor is carried out to determine the emissions of nitrogen oxides and carbon monoxide. Moreover, the effects of inlet temperature, flow rate, pressure, equivalence ratio, and humidity ratio over the emissions are investigated in this study. Based on the results, Increment of inlet temperature raises  $\text{NO}_x$  and reduces CO mass fractions. The maximum values of  $\text{NO}_x$  mass fractions of Fayetteville, Marcellus, Haynesville, and New Albany occurs at 0.98, 0.915, 1.03, and 1.03 equivalence ratios respectively. Rising humidity ratio of the burning air reduces  $\text{NO}_x$  and lightly uplifts CO mass fractions. Ascending inlet pressure grows up  $\text{NO}_x$  and mitigates CO mass fractions. Increasing inlet flow rate lowers  $\text{NO}_x$  and slightly enhances CO mass fractions.

**Keywords** Shale gas, combustion, nitrogen oxides, carbon monoxide

---

### 1. Introduction

Industrial progress, competition among countries, growing population and developing countries cause to the increase in energy demand in the last decay. Energy for vehicles, heating systems, industries and power plants is mostly obtained by combustion of carbon based fuels as gases, coals, oils, etc. Efficient combustion systems that produce energy by low fuels and emit less air pollutant have gained importance because of the effects of hazardous combustion emissions over human's health and environment [1].

The main gas pollutants emerging at the end of combustion because of incomplete combustion, high temperature, and fuel ingredient are nitrogen oxides ( $\text{NO}_x$ ), sulphur oxides ( $\text{SO}_x$ ), carbon monoxide (CO), hydrocarbons (HC), ozone ( $\text{O}_3$ ), and volatile organic compounds (VOCs) [2-5].  $\text{NO}_x$  consisting of mainly NO and  $\text{NO}_2$  causes diseases of respiratory system and is responsible for smog and acid rains with  $\text{SO}_x$  ( $\text{SO}$ , widely  $\text{SO}_2$ ) [6, 7]. HC constitutes the irritation at eye, nose and throat [2]. CO is a toxic gas and a reason for mortal poisoning. Finally,  $\text{O}_3$  and VOCs lead to respiration illness as asthma and allergic symptoms [8, 9]. Total emissions of CO,  $\text{NO}_x$ ,  $\text{SO}_2$ , and VOCs of USA in 2017 are determined as 60109, 10776, 2815, and 16232 in thousands of tons respectively [10]. World Health Organization has reported that seven million people die every year because of polluted air and ambient air pollution is the reason for the death of 4.2 million people in 2016 [11].

Shale gas consists of methane, heavy hydrocarbons (ethane, propane), carbon dioxide, nitrogen, hydrogen sulfide, and water. Shale gas has firstly begun to be extracted from shale rocks by horizontal drilling and hydraulic fracturing in USA. It is estimated that there is 100-year supply and shale gas will be %50 of total gas production by 2035 in USA. India, China, South Africa, UK, Poland, etc. are commercially about to evaluate their own shale gas resources. From environmental point of view, water polluted by hydraulic fracturing process, more greenhouse gas emitted by fleeing methane, and earthquake jeopardy caused by all extracting process stand as important issues [12, 13].



There are many studies over the combustion characteristics, the reduction of emissions, and emissions of natural gases under the conditions of laminar, turbulent, adiabatic, non-adiabatic, premixed, non-premixed, etc. in the literature. It is also seen that the compositions of some natural gases are close to the compositions of shale gases and researchers mostly focus on the emissions and environmental effects of the extracting process of shale gas. Vargas et al. determined adiabatic flame temperatures and laminar burning velocities in the combustion of several shale gas mixtures [13]. Cohen and Winkler detected the emission intensity between 0.31 tCO<sub>2</sub>/MWh and 0.59 tCO<sub>2</sub>/MWh at electricity production from shale gas in South Africa [14]. Chang et al. found the greenhouse gas emissions of shale gas to be lower than those of coal-fired electricity [15]. McTaggart-Cowan et al. concluded that nitrogen addition descends NO<sub>x</sub> emissions and ethane addition ascends it in high-pressure non-premixed natural gas combustion [16]. Zahedi and Yousefi determined the addition of N<sub>2</sub> or CO<sub>2</sub> to the mixture decreases NO emissions and the increasing initial pressures grows up NO emissions in pre-mixed laminar methane-air combustion [17]. Silva et al. studied on CO and CO<sub>2</sub> mass fractions in the emissions and temperature distributions for turbulent non-premixed combustion of natural gas in a cylindrical chamber [18]. Jerzak et al. concluded propane addition into natural gas increases CO concentration and causes a slight NO<sub>x</sub> rise in the combustion gas [19]. Hayashi et al. emphasized NO<sub>x</sub> ascends with pressure increment and high temperature in non-premixed gas combustion [20]. Boushaki et al. revealed that increasing equivalence ratio decreases NO<sub>x</sub> emissions, oxygen enrichment reduces CO emissions, and the flame temperature enhances NO<sub>x</sub> emissions for turbulent non-premixed methane combustion in a swirl burner [21]. Jerzak et al. concluded that the addition of CO<sub>2</sub> to natural gas rise CO emissions and leads to a reduction in NO<sub>x</sub> and the combustion temperature [22]. McTaggart-Cowan et al. extrapolated nitrogen addition to natural gas reduces the emissions of nitrogen oxides, particular matter, hydrocarbons, and carbon monoxide without affecting the performance and efficiency of a direct-injection engine [23].

In this study, air pollutant NO<sub>x</sub> and CO emissions of turbulent, non-premixed and non-adiabatic combustion of shale gas in a cylindrical burner are numerically determined under the effects of inlet pressure, temperature, flow rate, humidity ratio, and equivalence ratio by ANSYS software.

## 2. NO<sub>x</sub> and CO Formation

The formation of NO<sub>x</sub> occurs in the three ways called as thermal NO<sub>x</sub>, prompt NO<sub>x</sub>, and fuel NO<sub>x</sub> in a combustion process. Thermal NO<sub>x</sub> largely forms from nitrogen of the burning gas oxidizing with air via the thermal mechanism (Zeldovich) in the combustion chamber at high temperature over 1300 °C. Prompt NO<sub>x</sub> rapidly comes into existence when the formation rate of nitrogen oxides surpasses the oxidizing rate of nitrogen defined in thermal NO<sub>x</sub> in rich mixture region especially. Fuel NO<sub>x</sub> emerges from nitrogen in the fuel composition and generally depends on temperature, stoichiometry, the onset concentration of nitrogen in fuel/air mixture, etc. CO mostly arises from the join of carbon and oxygen atoms at the incomplete combustion of hydrocarbon fuels in the medium of low oxygen.

## 3. Methods

Combustion is a complex processes including thermo-dynamics, buoyancy, chemical kinetics, radiation, mass and heat transfers and fluid mechanics. Computer modeling and numerical solution of combustion are cheaper and easier to handle with respect to experimental way and consumes less time. It can be determined the flame composition, products, variation of temperature in the combustor for entered fuel compositions by Computational Fluid Dynamics (CFD) to study and analyze the combustion case [24].

**Table 1:** The shale gas compositions used in the numerical calculations [25]

| Regions      | CH <sub>4</sub> | C <sub>2</sub> H <sub>6</sub> | C <sub>3</sub> H <sub>8</sub> | CO <sub>2</sub> | N <sub>2</sub> |
|--------------|-----------------|-------------------------------|-------------------------------|-----------------|----------------|
| Marcellus    | 85.2            | 11.275                        | 2.875                         | 0.35            | 0.3            |
| Fayetteville | 97.3            | 1                             | 0                             | 1               | 0.7            |
| New Albany   | 89.875          | 1.125                         | 1.125                         | 7.875           | 0              |
| Haynesville  | 95              | 0.1                           | 0                             | 4.8             | 0.1            |

Fluent used for the calculations in this study is the computational fluid dynamic (CFD) software with finite volume method. It is also utilized for the solution of problems including fluid mechanics, heat transfer, combustion phenomenon, etc.



Shale gases used in the evaluation are extracted from different field sources of Marcellus, Fayetteville, New Albany, and Haynesville regions of USA. The average values of the gas compositions of the fields are given in Table 1.

The dimensions and wall temperature of the gas combustor and the inlet flow rates and temperatures of shale gas and air are depicted in Figure 1.

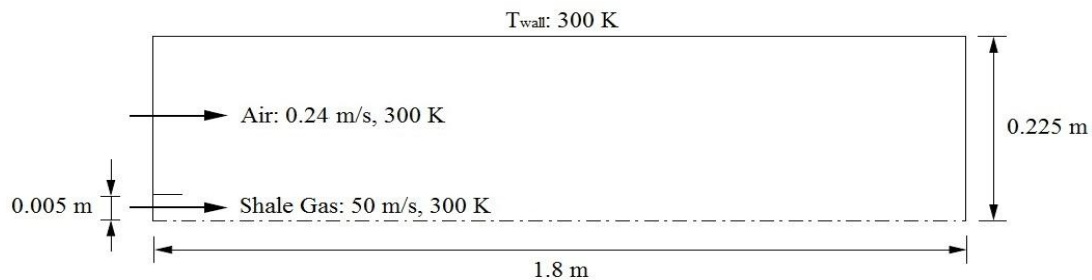


Figure 1: The cylindrical combustor and the inlet flow rates and temperatures [26]

The calculations of mass fraction of  $\text{NO}_x$  and CO emissions in shale gas/air combustions are performed in Fluid Flow (Fluent) from Analysis Systems of Ansys Workbench software. Fluent analysis the meshed geometry of a system and solves the equations of problem defined by mathematical models as laminar, turbulent, adiabatic, premixed, high-speed etc. with selected materials, boundary conditions, and solution controls. The mesh of the combustion field in two-dimension (2D) consists of 12261 nodes and 12000 elements. The following models and properties are chosen in the setup: Energy – On, Viscous Model – k-epsilon (2 eqn), k-epsilon model – standard, Near-Wall Treatment – Standart Wall Functions, Radiation Model – P1, Species Model – Non-Premixed Combustion (Inlet Diffusion, Chemical Equilibrium, Non-Adiabatic are selected),  $\text{NO}_x$  Model – On (Thermal, Prompt and  $\text{N}_2\text{O}$  Intermediate are selected). Low nitrogen of fuel is added from underOxid at Boundary tab of PDF Table by changing Fuel (shale gas) and Oxid(air) ratios and flow rates for the complete combustions and others.

#### 4. Results

The highest mass fraction of  $\text{NO}_x$  belongs to New Albany and Haynesville, Marcellus, and Fayetteville follow it in the decreasing order. Figure 2 shows  $\text{NO}_x$  mass fractions for all the shale gas combustion ascends with increasing inlet temperature of reactants. The temperature increment ascends thermal  $\text{NO}_x$  in the combustion chamber because increasing inlet temperatures raise the maximum reaction temperatures of all the shale gases. Thermal  $\text{NO}_x$  becomes dominant with regard to the prompt and fuel  $\text{NO}_x$  in high reaction temperatures. The  $\text{NO}_x$  increment between the emissions of combustions of New Albany and Haynesville at 255 and 315 K is around 39%. The percentage difference between these temperatures is about 36% for Marcellus and New Albany.

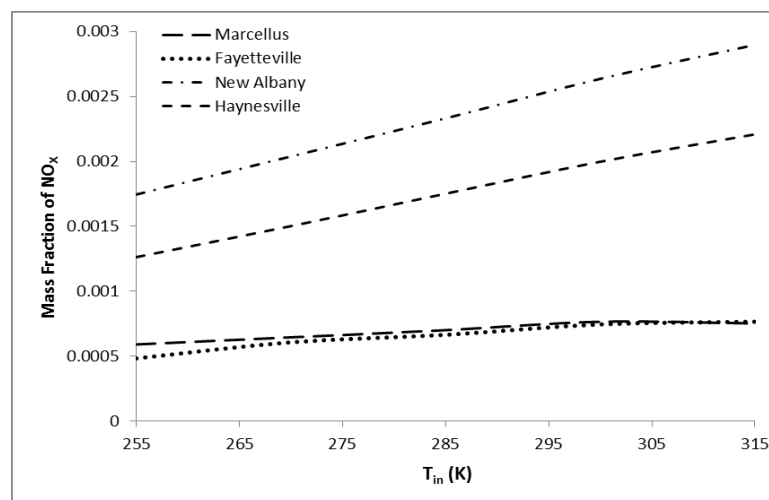


Figure 2: Variation of mass fraction of  $\text{NO}_x$  at different inlet temperature at  $ER=1$ ,  $P=1$  Bar,  $HR=0$



It can be seen in Figure 3 that the mass fractions of CO reduce with ascending inlet reactant temperature. The rank of mass fractions of CO from the highest to the lowest is Marcellus, Fayetteville, Haynesville, and New Albany. Increasing inlet temperature causes hydro-carbons to burn better in the burner with rising temperature and it descends CO mass fraction in the total. Variation of CO mass fraction is illustrated in Figure 4. The CO variation between the emissions of combustions of all the gases at 255 and 315 K is around 13%.

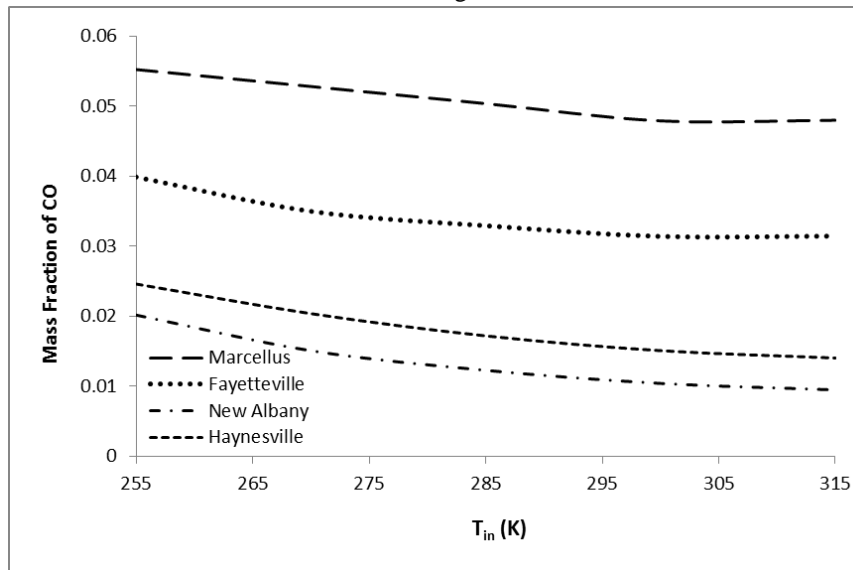


Figure 3: Variation of mass fraction of CO at different inlet temperature at  $ER=1$ ,  $P=1$  Bar,  $HR=0$

Variation of mass fraction of nitrogen oxides with respect to equivalence ratio is presented in Figure 4. The maximum  $NO_x$  for the combustions of Fayetteville, Marcellus, Haynesville, and New Albany occurs at the equivalence ratios of 0.98, 0.915, 1.03, and 1.03 respectively.  $NO_x$  emission of New Albany is the highest and 0.0027.

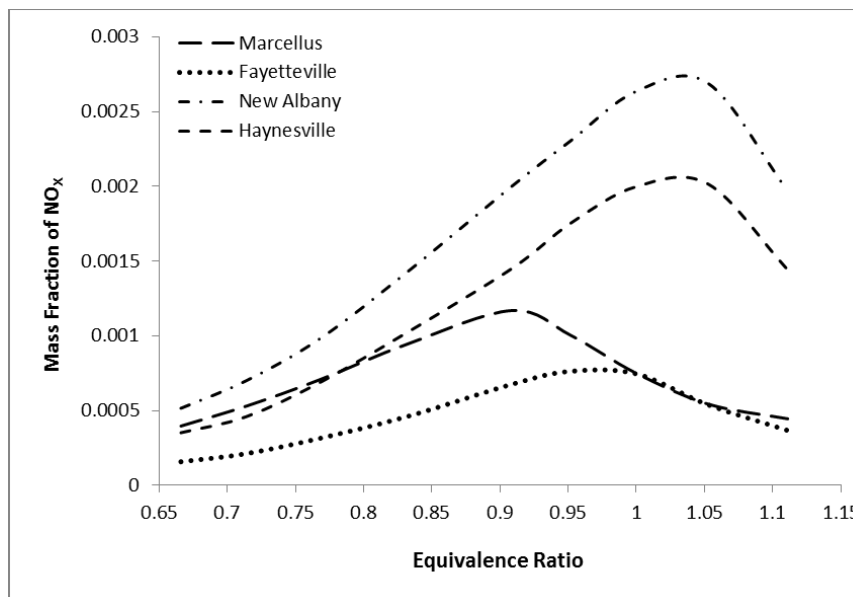


Figure 4: Variation of mass fraction of  $NO_x$  at different ERs at  $T_{in}=300$  K,  $P=1$  Bar,  $HR=0$

In Figure 5, increasing equivalent ratio enhances mass fraction of CO as expected. Ascending equivalence ratio means low burning air in the burner. This case causes the incomplete combustion of fuel stream and grows up CO emissions. The variation of CO emission between 0.666 and 1.111 of equivalence ratios is roughly 59.5% for Marcellus combustion.



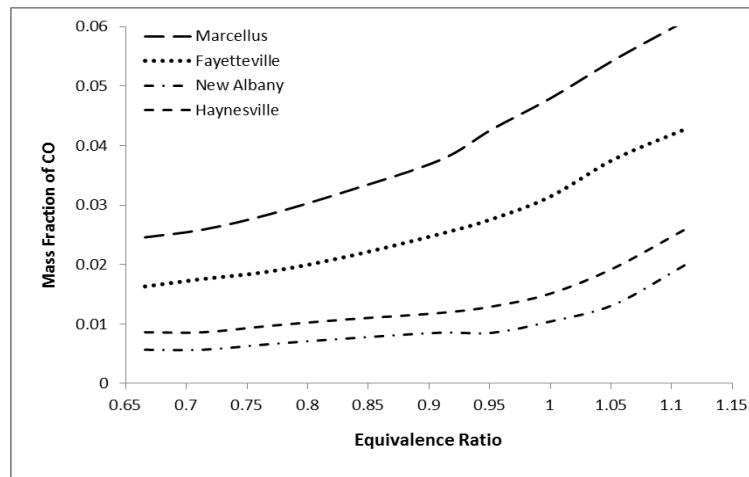


Figure 5: Variation of mass fraction of CO at different ER  $T_{in}=300$  K,  $P=1$  Bar,  $HR=0$

Figure 6 shows the augmentation of humidity in the burning air causes the temperature of reaction to decrease and the decreasing temperature leads to the reduction of  $NO_x$ . It is one of the ways to descend  $NO_x$  emissions.  $NO_x$  variation between 0 and 0.025 of humidity ratio is 46.6%, 48% and 61.8% in the descending tendency for New Albany, Haynesville, and the others respectively.

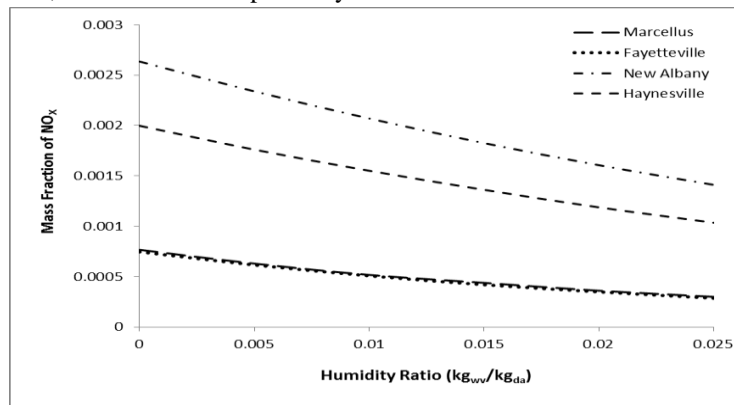


Figure 6: Variation of mass fraction of  $NO_x$  at different humidity ratio at  $ER=1$ ,  $T_{in}=300$  K,  $P=1$  Bar

It is given in Figure 7 that the augmentation of humidity in the burning air slightly raises mass fraction of CO. It points out the incomplete combustion of gases. The CO variations between 0 and 0.025 of humidity ratio are approximately 2%, 7.3%, 15%, and 13% for the combustions of Marcellus, Fayetteville, Haynesville, and New Albany.

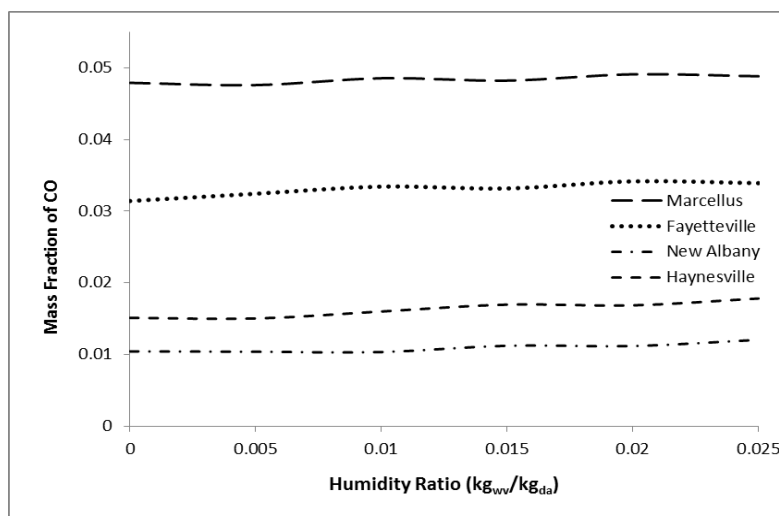


Figure 7: Variation of mass fraction of CO at different humidity ratio at  $ER=1$ ,  $T_{in}=300$  K,  $P=1$  Bar



The pressure measured by the gauge is relative to the atmospheric pressure as the zero point in the gas combustions. Rising inlet pressure raises mass fraction of  $\text{NO}_x$  for all the combustion, as given in Figure 8. The increment tendency is lower after the pressure of 2 bars.  $\text{NO}_x$  variations for 10 bars are around 50%, 56%, 75%, and 68.5% in the ascending tendency for New Albany, Haynesville, Marcellus and New Albany combustions.

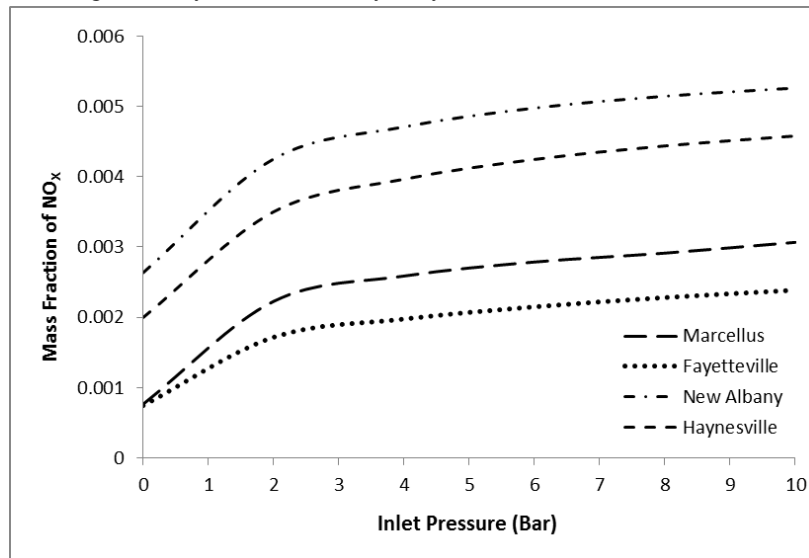


Figure 8: Variation of mass fraction of  $\text{NO}_x$  at different inlet pressure at  $ER= 1$ ,  $T_{in}=300\text{ K}$ ,  $HR=0$

Figure 9 shows the mass fraction of CO reduces till 2 bars, after that, it stays constant at the certain value. The CO variation for 10 Bar is about 7-9% for all the shale gas combustions. The highest value of CO belongs to Marcellus by 0.047.

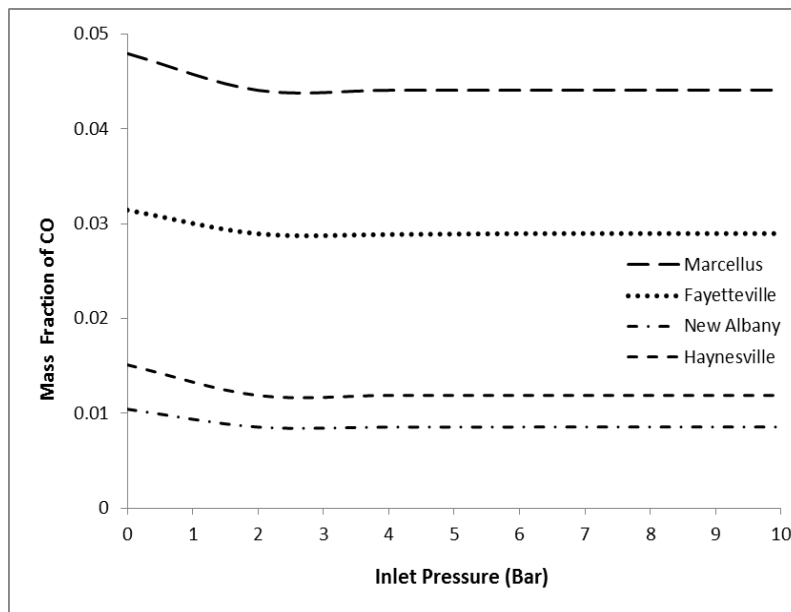


Figure 9: Variation of mass fraction of CO at different inlet pressure at  $ER= 1$ ,  $T_{in}=300\text{ K}$ ,  $HR=0$

Figure 10 indicates the variation of  $\text{NO}_x$  at the folds of different inlet flow rates. Escalating flow rates reduces the mass fraction of  $\text{NO}_x$ . High rates cause incomplete combustion because of entering excessive mass in the burner. Figure 11 shows it leads to the slight ascent of mass fraction of CO after 1.5 folds of flow rates.  $\text{NO}_x$  variations 1x and 3.5x folds of flow rates are 55.3%, 52.8%, 15.7%, and 39% in the decreasing tendency for New Albany, Haynesville, Marcellus, and New Albany combustions. The variations for CO mass fractions between 1x and 3.5x folds are 8-9% for all the combustions.



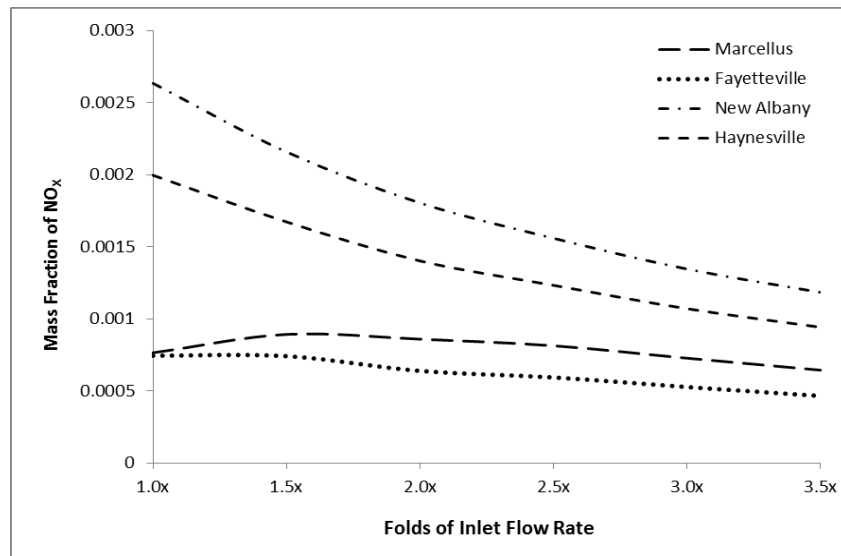


Figure 10: Variation of mass fraction of  $\text{NO}_x$  at folds of inlet flow rate at  $ER=1$ ,  $T_{in}=300\text{ K}$ ,  $P=1\text{ Bar}$ ,  $HR=0$

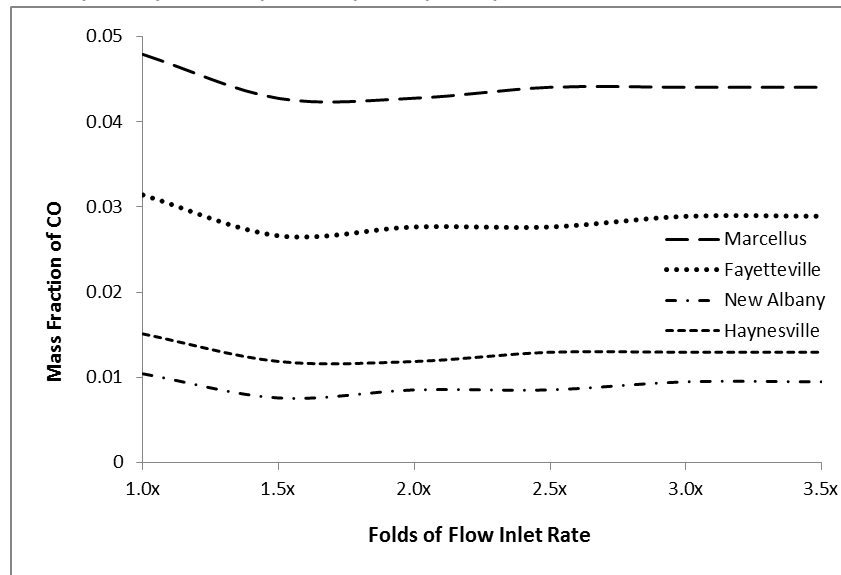


Figure 11: Variation of mass fraction of  $\text{CO}$  at folds of inlet flow rate at  $ER=1$ ,  $T_{in}=300\text{ K}$ ,  $P=1\text{ Bar}$ ,  $HR=0$

The emissions of  $\text{NO}_x$ ,  $\text{CO}$ ,  $\text{SO}_x$ , and the other pollutants in engines, power plants and heating systems including the gas combustion process are able to reduce to the acceptable levels by using the methods of water injection, compressed air, catalytic reduction, humid combustion air, exhaust gas re-circulation, low sulphur gas, liquid shower, etc.

## 5. Conclusion

The hazardous emissions of turbulent, non-premixed, and non-adiabatic combustions of four different shale gases extracted from various regions of USA are computationally investigated and the variations of mass fractions of  $\text{NO}_x$  and  $\text{CO}$  with disparate reactant inlet temperature, equivalence ratio, humidity ratio, inlet flow rate, and pressure are determined in this study. The following results are obtained:

- The mass fraction of  $\text{NO}_x$  increases with ascending reactant inlet temperatures for all the gases. The order of  $\text{NO}_x$  from the highest to the lowest is New Albany, Haynesville, Marcellus, and Fayetteville. The mass fraction of  $\text{CO}$  decreases with rising inlet temperatures. The rank of mass fractions of  $\text{CO}$  from the highest to the lowest is Marcellus, Fayetteville, Haynesville, and New Albany.



- The maximum NO<sub>x</sub> mass fractions for the combustions of Fayetteville, Marcellus, Haynesville, and New Albany arise at the equivalence ratios of 0.98, 0.915, 1.03, and 1.03. Ascending equivalent ratio raises the mass fraction of CO because of low burning air.
- Increasing humidity ratio causes the mass fractions of NO<sub>x</sub> to reduce. On the contrary, it lightly grows CO mass fractions.
- Ascending reactant inlet pressure raises NO<sub>x</sub> mass fractions. But, it reduces CO mass fractions until 2 bar. CO mass fractions stay constant after 2 bar.
- Rising reactant inlet flow rates diminish the mass fractions of NO<sub>x</sub> and slightly increases CO mass fractions.

The high emissions of nitrogen oxides and carbon monoxide emerging under the given combustion conditions could be brought under control at an acceptable level by using some methods as water injection, catalytic reduction, exhaust gas re-circulation, etc. in the gas combustion systems.

### References

- [1]. Byeonghun, Y., Seungro, L., & Chang-Eon, L. (2015). Study of NO<sub>x</sub> emission characteristics in CH<sub>4</sub>/air non-premixed flames with exhaust gas recirculation. *Energy*, 91: 119-127.
- [2]. Wojciech, J. (2014). Emissions of NO<sub>x</sub> and CO from natural gas combustion with adding CO<sub>2</sub> at varying distances from the burner. *Middle Pomeranian Scientific Society of the Environment Protection*, 16: 148-160.
- [3]. Michael Alberts, W. (1994). Indoor air pollution: NO, NO<sub>2</sub>, CO, and CO<sub>2</sub>. *J Allergy Clin Immunol*, 94: 289-295.
- [4]. Pénard-Morand, C., & Annesi-Maesano, I. (2004). Air pollution: from sources of emissions to health effects. *Breathe*, 1(2): 109-119.
- [5]. Bocola, W., & Cirillo, M. C. (1989). Air pollutant emissions by combustion processes in Italy. *Atmospheric Environment*, 23(1): 17-24.
- [6]. Kalel, M., Choudhary, R., & Dixit, S. K. (2015). A computational evaluation of emissions for non-premixed natural gas combustion. *International Journal of Scientific Research Engineering & Technology*, 4(7), 731-735.
- [7]. Somarathne, K. D. K. A., Parwatha, G., Oguri, S., Nada, Y., Ito, T., & Noda, S. (2013). NO<sub>x</sub> reduction of non-premixed flames by combination of burner and furnaces. *Journal of Environment and Engineering*, 8(1):1-10.
- [8]. Akça, H., Ürel, G., Karacan, C. D., Tuygun, N., & Polat, E. (2017). The effect of carbon monoxide poisoning on platelet volume in children. *J Pediatr Emerg Intensive Care Med*, 4:13-16.
- [9]. Alyüz, B., & Veli, S. (2006). İçörtamhavasındabulunanauçucuorganikbileşiklervesağlıküzerineetkileri. *TrakyaUniv J Sci*, 7(2): 109–116.
- [10]. United States Environmental Protection Agency (EPA), Air Pollutant Emissions, [https://www.epa.gov/air-emissions-inventories/air-pollutant-emissions-trends-data1970\\_2017](https://www.epa.gov/air-emissions-inventories/air-pollutant-emissions-trends-data1970_2017), 15.11.2018.
- [11]. World Health Organization, Air Pollutants (WHO), <http://www.who.int/news-room/air-pollution>, 15.11.2018.
- [12]. Wang, Q., Chen, X., Jha, A. N., & Rogers, H. (2014). Natural gas from shale formation-the evolution, evidences and challenges of shale gas revolution in United States. *Renewable and Sustainable Energy Reviews*, 30:1-28.
- [13]. Vargas, A. C., Arrieta, A. A., & Arrieta, C. E. (2016). Combustion characteristics of several typical shale gas mixtures. *Journal of Natural Gas Science and Engineering*, 33:296-304.
- [14]. Cohen, B., & Winkler, H. (2014). Greenhouse gas emissions from shale gas and coal for electricity generation in South Africa. *S Afr J Sci.*, 110(3/4): 1-5.
- [15]. Chang, Y., Huang, R., Ries, R. J., & Masanet, E. (2015). Life-cycle comparison of greenhouse gas emissions and water consumption for coal and shale gas fired power generation in China. *Energy*, 86:335-343.





- [16]. McTaggart-Cowan, G. P., Wu, N., Jin, B., Rogak, S. N., Davy, M. H. & Bushe, W. K. (2009). Effects of fuel composition on high-pressure non-premixed natural gas combustion. *Combustion Science and Technology*, 181: 397-416.
- [17]. Zahedi, P., & Yousefi, K. (2014). Effects of pressure and carbon dioxide, hydrogen and nitrogen concentration on laminar burning velocities and NO formation of methane-air mixtures. *Journal of Mechanical Science and Technology*, 28(1): 377-386.
- [18]. Silva, C. V., Franca, F. H. R., & Vielmo, H. A. (2007). Analysis of the turbulent, non-premixed combustion of natural gas in a cylindrical chamber with and without thermal radiation. *Combust. Sci. and Tech.*, 179: 1605-1630.
- [19]. Jerzak, W., Kalicka, Z., & Kawecka-Cebula, E. (2015). On CO and NO<sub>x</sub> emission in the kinetic combustion of propane/natural gas mixtures. *Environment Protection Engineering*, 41(3): 87-100.
- [20]. Hayashi, S., Yamada, H., Shimodaira, K., & Machida, T. (1998). NO<sub>x</sub> emissions from non-premixed, direct fuel injection methane burners at high-temperature and elevated pressure conditions. *Twenty-Seventh Symposium (International) on Combustion/The Combustion Institute*, 1833–1839.
- [21]. Boushakia, T., Merloa, N., Chauveaua, C., & Gökalp, I. (2017). Study of pollutant emissions and dynamics of non-premixed turbulent oxygen enriched lames from a swirl burner. *Proceedings of the Combustion Institute*, 36: 3959–3968.
- [22]. Jerzak, W., Kuzniaa, M., & Zajemska, M. (2014). The effect of adding CO<sub>2</sub> to the axis of natural gas combustion flames on CO and NO<sub>x</sub> concentrations in the combustion chamber. *Journal of Power Technologies*, 94:(3), 202–210.
- [23]. McTaggart-Cowan, G. P., Rogak, S. N., Hill, P. G., Munshi, S. R., & Bushe, W. K. (2007). The effects of fuel dilution in a natural-gas direct-injection engine. *Proceedings of the Institution of Mechanical Engineers, Part D: Journal of Automobile Engineering*, 222(3): 441-453.
- [24]. Guessab, A., Aris, A., & Bounif, A. (2013). Simulation of turbulent piloted methane non-premixed flame based on combination of finite-rate/eddy-dissipation model. *Mechanika*, 19:(6) 657-664.
- [25]. Bullin, K., Krouskop, P., & Bryan, Research and Engineering Inc. Bryan, Tex. (2008). Composition variety complicates processing plans for US shale gas. E-book, Based on: Annual Forum, Gas Processors Association, Houston Chapter, Houston.
- [26]. ANSYS Release 12.0. (2009). Tutorial 14. Modeling species transport and gaseous combustion. 1-46, ANSYS, Inc.

